

UCLA

UCLA Previously Published Works

Title

Methyltransferase Dnmt3a upregulates HDAC9 to deacetylate the kinase TBK1 for activation of antiviral innate immunity.

Permalink

<https://escholarship.org/uc/item/4d45q23q>

Journal

Nature immunology, 17(7)

ISSN

1529-2908

Authors

Li, Xia
Zhang, Qian
Ding, Yuanyuan
et al.

Publication Date

2016-07-01

DOI

10.1038/ni.3464

Peer reviewed

Methyltransferase Dnmt3a upregulates HDAC9 to deacetylate the kinase TBK1 for activation of antiviral innate immunity

Xia Li^{1,2,6}, Qian Zhang^{2,3,6}, Yuanyuan Ding^{1,6}, Yiqi Liu¹, Dezhi Zhao¹, Kai Zhao², Qicong Shen³, Xingguang Liu³, Xuhui Zhu³, Nan Li³, Zhongyi Cheng⁴, Guoping Fan⁵, Qingqing Wang¹ & Xuetao Cao¹⁻³

The DNA methyltransferase Dnmt3a has high expression in terminally differentiated macrophages; however, its role in innate immunity remains unknown. Here we report that deficiency in Dnmt3a selectively impaired the production of type I interferons triggered by pattern-recognition receptors (PRRs), but not that of the proinflammatory cytokines TNF and IL-6. Dnmt3a-deficient mice exhibited enhanced susceptibility to viral challenge. Dnmt3a did not directly regulate the transcription of genes encoding type I interferons; instead, it increased the production of type I interferons through an epigenetic mechanism by maintaining high expression of the histone deacetylase HDAC9. In turn, HDAC9 directly maintained the deacetylation status of the key PRR signaling molecule TBK1 and enhanced its kinase activity. Our data add mechanistic insight into the crosstalk between epigenetic modifications and post-translational modifications in the regulation of PRR signaling and activation of antiviral innate immune responses.

Epigenetic regulation is important for myeloid-cell development and innate immune responses, especially for modulation of the chromatin status at loci encoding Toll-like receptors (TLRs) and signaling regulators and the transcription of genes encoding inflammatory products, mediated by transcription factors of the NF- κ B family^{1,2}. Histone modifications and chromatin remodeling are reported to mediate largely gene-specific regulation of both the initial induction of the transcription of cytokine-encoding genes during pathogen infection and transcriptional repression in tolerant innate cells for the resolution of inflammation³⁻⁶. As a stable transcriptional silencer, DNA methylation has an important role in maintaining genome stability and regulating gene expression⁷. However, the role of DNA methylation in regulating innate immunity has remained elusive. Moreover, although epigenetic regulation of TLR signaling and inflammatory cytokines in innate immunity has been revealed, the chromatin regulators involved in antiviral innate signaling are largely unknown.

Enzymes for adding or erasing post-translational modifications (PTMs) act as vital regulators of cellular signal transduction during innate immune responses⁸⁻¹⁰. The acetylation of lysine residues in histone and non-histone proteins and the enzymes involved in this are well appreciated¹¹. In the development and function of the innate immune system, lysine acetylation, which affects the stability, activation and subcellular localization of proteins and the interaction of proteins with other proteins or DNA, has been identified as a critical

regulator⁹. Several non-histone proteins that are signal transducers important for 'fine-tuning' TLR pathways¹² and transcriptional regulators of the expression of inflammatory cytokines^{13,14} are regulated by acetylation. However, only a few targets of lysine acetylation in the innate immune response have been discovered; additional functions of the acetylation of non-histone proteins, such as crosstalk with conventional PTMs and modulation of the kinase activity of signaling transducers in the innate immune response, remain to be revealed.

The kinase TBK1 is required for activation of the transcription factor IRF3 and subsequent induction of expression of type I interferons in antiviral signaling¹⁵⁻¹⁷. The active state of TBK1 is tightly regulated by PTMs such as phosphorylation and ubiquitination, and positive and negative regulators of these two PTMs have been identified¹⁸⁻²⁰. However, role of unconventional PTMs such as acetylation in regulating the activation and kinase activity of TBK1 remains unknown.

Many unconventional PTM regulators are also chromatin modifiers, which indicates that there might be crosstalk between the epigenetic regulation of transcription and the PTM of signal transducers during innate response. According to the database of the gene-annotation portal BioGPS²¹ and our preliminary data, macrophages have high expression of the DNA methyltransferase Dnmt3a, but so far the role of DNA methylation in regulating innate responses has remained largely unknown. To explore the biological importance of high expression of Dnmt3a in innate immunity, we conditionally deleted *Dnmt3a*

¹Institute of Immunology, Zhejiang University School of Medicine, Hangzhou, China. ²National Key Laboratory of Medical Molecular Biology & Department of Immunology, Institute of Basic Medical Sciences, Peking Union Medical College, Chinese Academy of Medical Sciences, Beijing, China. ³National Key Laboratory of Medical Immunology & Institute of Immunology, Second Military Medical University, Shanghai, China. ⁴Advanced Translational Medicine Institute, Tongji University, Shanghai, China. ⁵Department of Human Genetics, David Geffen School of Medicine, University of California Los Angeles, California, USA. ⁶These authors contributed equally to this work. Correspondence should be addressed to X.C. (caoxt@immunol.org) or Q.W. (wqq@zju.edu.cn).

Received 9 November 2015; accepted 12 April 2016; published online 30 May 2016; corrected online 9 June 2016 (details online); doi:10.1038/ni.3464

in macrophages and found that Dnmt3a selectively upregulated production of the type I interferons IFN- α and IFN- β by maintaining high expression, in macrophages, of the histone deacetylase HDAC9, which directly enhanced the activation of TBK1 by deacetylating it in response to the innate stimuli. Our results provide mechanistic insight into the epigenetic modulation of antiviral innate responses and identify a previously unknown manner whereby unconventional PTMs regulate the kinase activity of TBK1.

RESULTS

Dnmt3a deficiency selectively impairs type I interferon production

Inspired by published gene-expression profiles of mouse peritoneal macrophages²², we analyzed the expression of genes encoding Dnmt enzymes and found that among these, *Dnmt3a* had the highest expression in mouse peritoneal macrophages (Fig. 1a,b). Mouse peritoneal macrophages had the highest expression of Dnmt3a (both mRNA and protein) among the immune cells analyzed, including CD4⁺ or CD8⁺ T cells, B cells, mast cells, natural killer cells and dendritic cells (Fig. 1c,d). To investigate whether Dnmt3a has a role in innate immunity, we generated *Dnmt3a*^{fl/fl}*Lyz2*-Cre mice, which undergo deletion of *loxP*-flanked *Dnmt3a* alleles (*Dnmt3a*^{fl/fl}) specifically in myeloid cells

via Cre recombinase expressed from the myeloid cell-specific gene *Lyz2* (*Lyz2*-Cre) (Supplementary Fig. 1a). *Dnmt3a*^{fl/fl}*Lyz2*-Cre mice had normal differentiation and numbers of peritoneal macrophages (Supplementary Fig. 1b–d). We found that expression of the type I interferons IFN- α and IFN- β (both mRNA and protein), but not that of the proinflammatory cytokines TNF or IL-6, induced by lipopolysaccharide (LPS) (a TLR4 ligand), the synthetic RNA duplex poly(I:C) (a TLR3 ligand), the synthetic double-stranded DNA poly(dA:dT) or poly(dG:dC) or cGAMP (ligands in the DNA-sensing pathway), the RNA viruses vesicular stomatitis virus (VSV) or Sendai virus (SeV), or the DNA virus herpes simplex virus type 1 (HSV-1) was significantly lower in *Dnmt3a*-deficient (*Dnmt3a*^{fl/fl}*Lyz2*-Cre) peritoneal macrophages than in their *Dnmt3a*-sufficient (*Dnmt3a*^{fl/fl}) counterparts (Fig. 1e,f). However, the expression of IFN- α , IFN- β , TNF and IL-6 (both mRNA and protein) remained unchanged in *Dnmt3a*-deficient peritoneal macrophages stimulated with CpG oligodeoxynucleotide (ODN) (a TLR9 ligand) (Fig. 1e,f). Accordingly, knockdown of Dnmt3a via small interfering RNA (siRNA) also substantially reduced the expression of IFN- α and IFN- β (both mRNA and protein), but not that of TNF or IL-6, induced by LPS, poly(I:C), VSV, SeV or HSV-1 in peritoneal macrophages (Supplementary Fig. 2a,b), whereas the expression of IFN- α , IFN- β , TNF and IL-6 (both mRNA and protein) remained unchanged in peritoneal macrophages stimulated with CpG ODN after siRNA-mediated knockdown of Dnmt3a (Supplementary Fig. 2c,d). Furthermore, knockdown of Dnmt3a barely

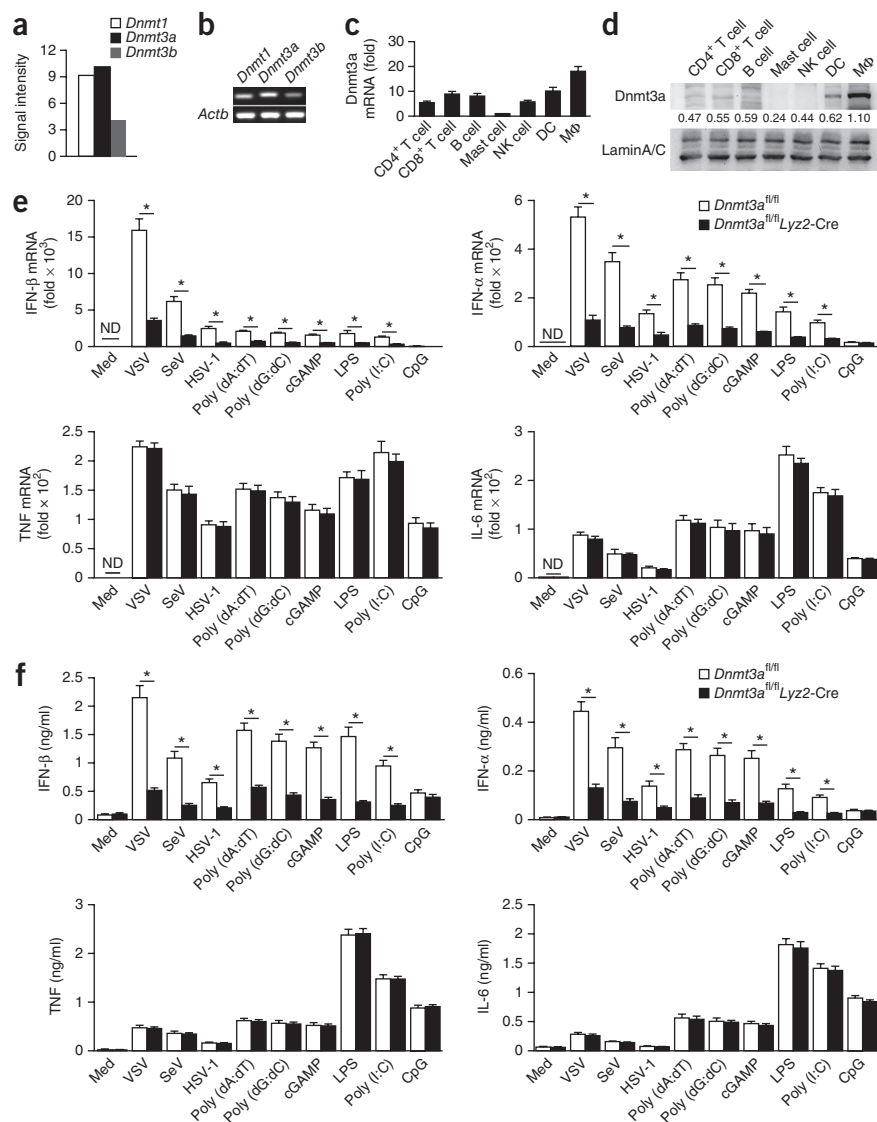


Figure 1 Deficiency in Dnmt3a selectively impairs the production of type I interferons. (a) Microarray analysis of *Dnmt1*, *Dnmt3a* and *Dnmt3b* in mouse peritoneal macrophages in the absence of innate stimuli. (b) Quantitative PCR and gel-electrophoresis analysis of *Dnmt1*, *Dnmt3a* and *Dnmt3b* in peritoneal macrophages; the reference gene *Actb* (which encodes β -actin) serves as a loading control. (c) Quantitative PCR analysis of Dnmt3a mRNA in mouse immune cells; results were normalized to those of β -actin mRNA. NK cell, natural killer cell; DC, dendritic cell; M Φ , macrophage. (d) Immunoblot analysis of Dnmt3a and lamin A/C (loading control throughout) in mouse immune cells; numbers below lanes indicate densitometry of Dnmt3a relative to that of lamin A/C. (e) Quantitative PCR analysis of IFN- β , IFN- α , TNF and IL-6 mRNA in *Dnmt3a*^{fl/fl} or *Dnmt3a*^{fl/fl}*Lyz2*-Cre peritoneal macrophages treated for 8 h with medium alone (Med), infected for 8 h with VSV, SeV or HSV-1, or stimulated for 4 h with poly(dA:dT), poly(dG:dC) or cGAMP (all analyses) or for 2 h (analysis of IFN- β , IFN- α and TNF) or 4 h (analysis of IL-6) with LPS, poly(I:C) or CpG ODN. (f) ELISA of IFN- β , IFN- α , TNF and IL-6 in supernatants of *Dnmt3a*^{fl/fl} and *Dnmt3a*^{fl/fl}*Lyz2*-Cre peritoneal macrophages infected for 12 h with VSV, SeV or HSV-1 or stimulated for 12 h with poly(dA:dT), poly(dG:dC) or cGAMP or for 8 h with LPS, poly(I:C) or CpG ODN. ND, not detectable. * P < 0.01 (two-tailed Student's *t*-test). Data are representative of three experiments (a) or three independent experiments with similar results (b,d) or are from three independent experiments (c,e,f; mean \pm s.e.m.).

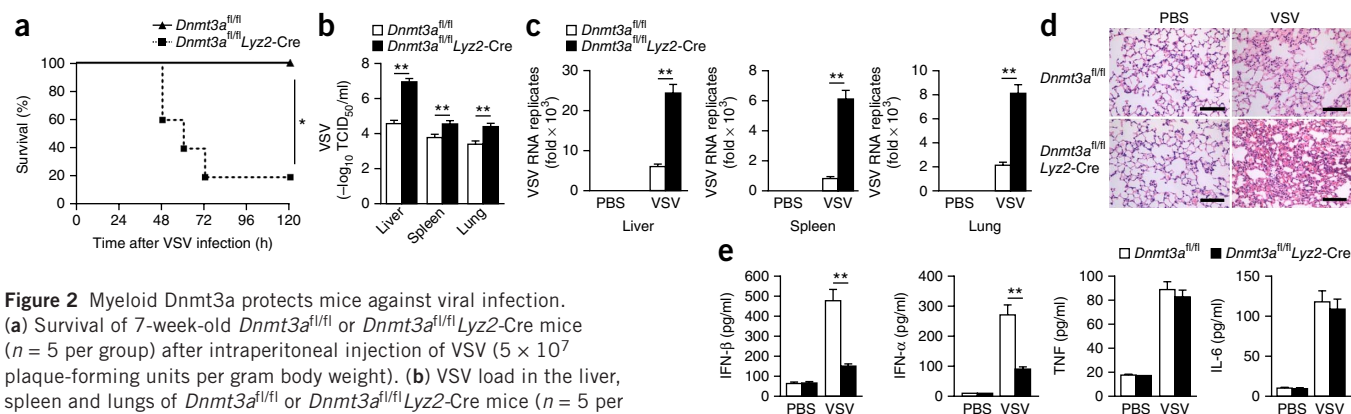


Figure 2 Myeloid Dnmt3a protects mice against viral infection. (a) Survival of 7-week-old *Dnmt3a^{fl/fl}* or *Dnmt3a^{fl/fl}Lyz2-Cre* mice ($n = 5$ per group) after intraperitoneal injection of VSV (5×10^7 plaque-forming units per gram body weight). (b) VSV load in the liver, spleen and lungs of *Dnmt3a^{fl/fl}* or *Dnmt3a^{fl/fl}Lyz2-Cre* mice ($n = 5$ per group) 24 h after infection with VSV (as in a), assessed by endpoint-dilution assay and presented as 50% tissue culture infectious dose (TCID₅₀). (c) Quantitative PCR analysis of VSV RNA in the liver, spleen and lungs of *Dnmt3a^{fl/fl}* or *Dnmt3a^{fl/fl}Lyz2-Cre* mice 24 h after intraperitoneal injection of PBS or VSV (as in a). (d) Hematoxylin-and-eosin staining of sections of lungs from mice as in c. Scale bars, 50 μ m. (e) ELISA of cytokines in serum from mice as in c. * $P < 0.05$ and ** $P < 0.01$ (Kaplan-Meier (a) or two-tailed Student's t -test (b,c,e)). Data are representative of three independent experiments with similar results (a,d) or are from three independent experiments (b,c,e; mean \pm s.e.m.).

affected the HSV-1-induced expression of IFN- α mRNA or IFN- β mRNA in L929 mouse fibroblasts stably expressing a short hairpin RNA (shRNA) directed against the membrane-associated adaptor STING (Supplementary Fig. 2e). However, expression of IFN- β mRNA and IFN- α mRNA was impaired in L929 cells stably expressing shRNA directed against STING when Dnmt3a was transiently knocked down via shRNA, followed by infection with VSV or SeV (Supplementary Fig. 2e). Thus, Dnmt3a was able to selectively upregulate the TBK1-dependent production of type I interferons triggered by TLR3 and TLR4 and viruses.

Myeloid Dnmt3a protects mice against viral infection

To further elucidate the importance of Dnmt3a in antiviral immunity, we challenged *Dnmt3a^{fl/fl}Lyz2-Cre* mice with the RNA virus VSV and found that the mortality of these Dnmt3a-deficient mice was greater than that of their Dnmt3a-sufficient (*Dnmt3a^{fl/fl}*) littermates (Fig. 2a). VSV titers and VSV replication in various organs were also significantly greater in Dnmt3a-deficient mice than in their Dnmt3a-sufficient counterparts (Fig. 2b,c), and there was more infiltration of inflammatory cells into the lungs of Dnmt3a-deficient mice than in those of their Dnmt3a-sufficient counterparts following infection (Fig. 2d). Dnmt3a-deficient mice produced much less IFN- α and IFN- β in serum than did their Dnmt3a-sufficient littermates in response to infection with VSV (Fig. 2e). Therefore, Dnmt3a was required for the efficient production of type I interferons and for the resistance of these mice to viral infection.

Deficiency in Dnmt3a impairs phosphorylation of IRF3

Next we investigated the mechanisms underlying Dnmt3a's activity in promoting the production of type I interferons. Dnmt3a did not bind to the promoter of the gene encoding IFN- β (*Ifnb1*), nor was DNA methylation of the *Ifnb1* promoter altered during VSV infection (Supplementary Fig. 3a,b), which excluded the possibility that Dnmt3a directly regulated transcription of the gene encoding IFN- β . We then screened the signaling pathways responsible for initiating the production of type I interferons. Phosphorylation of the transcription factor IRF3 at Ser396 is strongly correlated with its full activation²³. We found less phosphorylation of IRF3 at Ser396 induced by VSV, LPS or cGAMP in Dnmt3a-deficient (*Dnmt3a^{fl/fl}Lyz2-Cre*) peritoneal macrophages than in their Dnmt3a-sufficient (*Dnmt3a^{fl/fl}*) counterparts (Fig. 3a-c). Accordingly, IRF3 phosphorylated at Ser396 was diminished

in peritoneal macrophages in which Dnmt3a was knocked down and that were infected with VSV or stimulated with LPS, relative to that in similarly treated cells in which Dnmt3a was not knocked down (Supplementary Fig. 4a,b). Similarly, dimerization of IRF3 was also lower in Dnmt3a-deficient peritoneal macrophages infected with VSV or stimulated with LPS or cGAMP than in their Dnmt3a-sufficient counterparts (Fig. 3d-f), and deficiency in Dnmt3a resulted in less VSV-, LPS- or cGAMP-induced translocation of IRF3 to the nucleus (Fig. 3g-i). Furthermore, deficiency in Dnmt3a decreased the amount of IRF3 at the promoter region of *Ifnb1* (Fig. 3j). As noted above, TBK1 is essential for optimal IRF3 activation¹⁵. Unexpectedly, phosphorylation of TBK1 was barely affected by a decrease in or total deficiency in Dnmt3a in peritoneal macrophages (Fig. 3a-c). In addition, a decrease in or total deficiency in Dnmt3a barely affected the NF- κ B and mitogen-activated protein kinase signaling pathways in peritoneal macrophages infected with VSV or stimulated with LPS (Supplementary Fig. 4c-f). Together these results indicated that Dnmt3a was required for PRR-triggered activation of IRF3 and the production of type I interferons.

Dnmt3a maintains expression of HDAC9

TBK1 is critical for proper IRF3 activation^{24,25}. Dnmt3a selectively promoted the phosphorylation of IRF3 but not that of TBK1, indicative of an alternative mechanism for the regulation of TBK1 activation by Dnmt3a. To elucidate the underlying mechanism by which Dnmt3a enhanced the TBK1-mediated activation of IRF3, we used gene-chip analysis to assess the gene-expression profile of peritoneal macrophages in which Dnmt3a was knocked down in the absence of innate stimuli and found that knockdown of Dnmt3a affected the expression of hundreds of genes (Supplementary Table 1). The microarray data indicated that 338 genes were downregulated and 289 genes were upregulated in peritoneal macrophages in which Dnmt3a was knocked down (Supplementary Table 1). The large number of downregulated genes in peritoneal macrophages in which Dnmt3a was knocked down suggested that although Dnmt3a-mediated DNA methylation is usually associated with gene silencing, Dnmt3a might also have a positive role in driving transcription. Further, the binding of Dnmt3a to DNA might be used together with DNA methylation to maintain active chromatin states by antagonizing silencing modifications, such as that seen with trimethylation of histone H3 at Lys27 (H3K27me3) in specific lineage commitment²⁶. Among the five genes

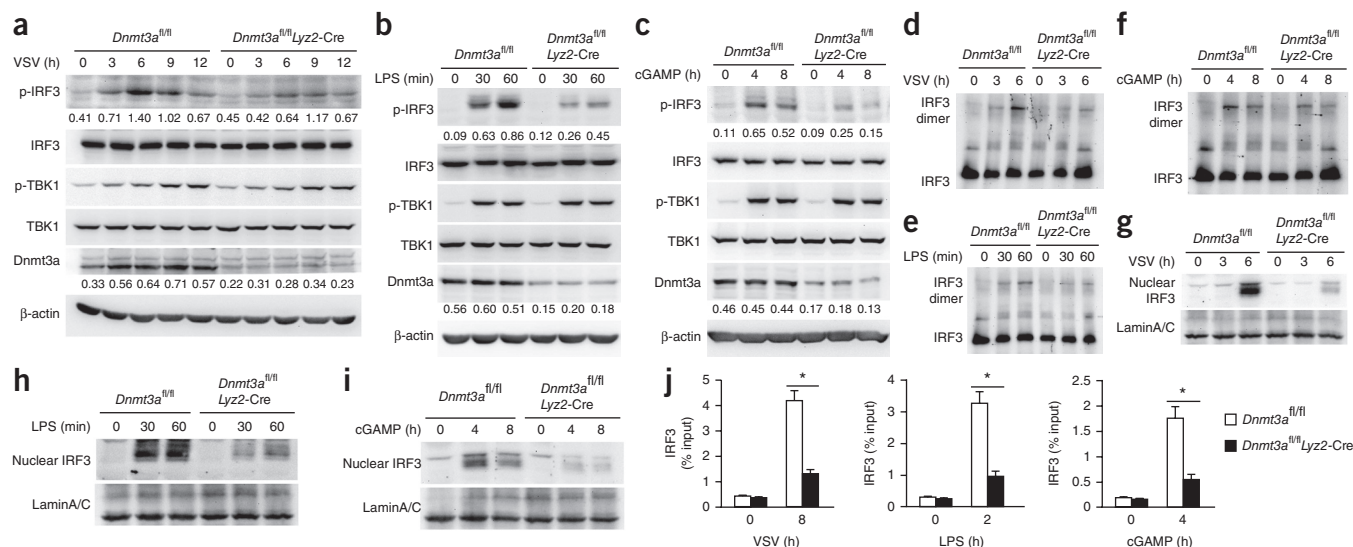
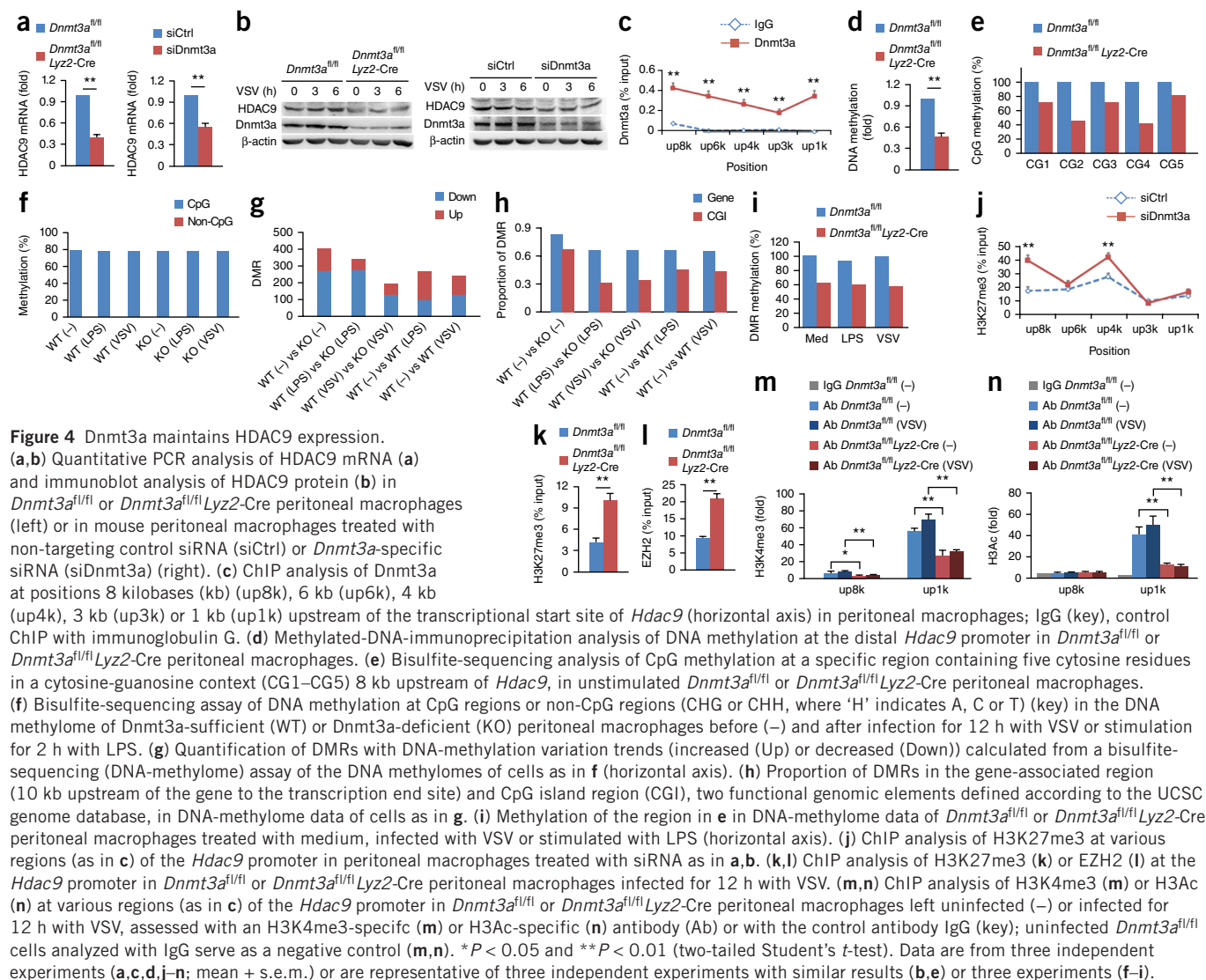


Figure 3 Deficiency in *Dnmt3a* impairs IRF3 phosphorylation. (a–c) Immunoblot analysis of phosphorylated (p-) or total IRF3, TBK1 and *Dnmt3a* (left margins) or β -actin (loading control throughout) in *Dnmt3a*^{fl/fl} or *Dnmt3a*^{fl/fl} *Lyz2-Cre* peritoneal macrophages infected for various times (above lanes) with VSV (a) or stimulated for various times (above lanes) with LPS (b) or cGAMP (c); numbers below lanes indicate densitometry of phosphorylated IRF3 or total *Dnmt3a* relative to that of β -actin. (d–f) Immunoblot analysis of IRF3 dimerization in *Dnmt3a*^{fl/fl} or *Dnmt3a*^{fl/fl} *Lyz2-Cre* peritoneal macrophages infected for various times (above lanes) with VSV (d) or stimulated for various times (above lanes) with LPS (e) or cGAMP (f). (g–i) Immunoblot analysis of IRF3 among nuclear proteins in *Dnmt3a*^{fl/fl} or *Dnmt3a*^{fl/fl} *Lyz2-Cre* peritoneal macrophages infected for various times (above lanes) with VSV (g) or stimulated for various times (above lanes) with LPS (h) or cGAMP (i). (j) ChIP analysis of IRF3 at the *Irfn1* promoter in *Dnmt3a*^{fl/fl} or *Dnmt3a*^{fl/fl} *Lyz2-Cre* peritoneal macrophages infected for 0 or 8 h (horizontal axis) with VSV (left) or stimulated for 0, 2 or 4 h (horizontal axes) with LPS (middle) or cGAMP (right). **P* < 0.01 (two-tailed Student's *t*-test). Data are representative of three independent experiments with similar results (a–i) or are from three independent experiments (j; mean + s.e.m.).

that were the most downregulated or upregulated, we identified three candidates for further analysis: the genes encoding the kinase *Nek2*, *HDAC9*, and the enzyme *Madd*. We also assessed gene expression in naive *Dnmt3a*-deficient peritoneal macrophages by high-throughput sequencing technologies (RNA-seq). Although *Dnmt3a* is essential for lineage commitment, RNA-seq analysis showed that loss of *Dnmt3a* barely decreased the transcription of genes encoding PRRs or signaling transducers listed in the KEGG (Kyoto Encyclopedia of Genes and Genomes) database²⁷ (Supplementary Table 2). Only transcription of the gene encoding the ubiquitin-like modifier *ISG15* was upregulated in *Dnmt3a*-deficient naive peritoneal macrophages relative to its expression in their *Dnmt3a*-sufficient counterparts (Supplementary Table 2), probably due to a feedback effect of impaired TBK1-IRF3 signaling. Among the three candidates, only the gene encoding *HDAC9* displayed an mRNA-variation pattern similar to that in cells in which *Dnmt3a* was silenced; the other two did not seem to be dysregulated (Supplementary Table 2), a result possibly caused by compensation for constitutive loss of *Dnmt3a*.

Next we confirmed the role of *Dnmt3a* in maintaining *HDAC9* expression. Knockdown of *Dnmt3a* and deficiency in *Dnmt3a* were found to significantly inhibit *HDAC9* expression in peritoneal macrophages (Fig. 4a,b). As an epigenetic modifier, *Dnmt3a* in most cases binds directly to the gene to regulate transcription^{28–30}. Accordingly, by chromatin-immunoprecipitation (ChIP) assay, we found *Dnmt3a* directly bound to both proximal promoters and distal promoters of *Hdac9* in peritoneal macrophages in the absence of innate stimuli (Fig. 4c). Furthermore, we analyzed the methylation state of the distal *Hdac9* promoter by methylated-DNA immunoprecipitation and found less methylation in *Dnmt3a*-deficient peritoneal macrophages than in their *Dnmt3a*-sufficient counterparts (Fig. 4d). We further assessed methylation at the level of single CpG dinucleotides and found several CpG dinucleotides at the distal *Hdac9* promoter with

less methylation in *Dnmt3a*-deficient peritoneal macrophages than in their *Dnmt3a*-sufficient counterparts (Fig. 4e). As *Dnmt3a* is the key DNA methyltransferase, we established the base-resolution pattern of DNA methylation ('DNA methylome') of *Dnmt3a*-sufficient and *Dnmt3a*-deficient peritoneal macrophages before and after infection with VSV or stimulation with LPS. In mouse peritoneal macrophages, only cytosine residues in a cytosine-guanine context were methylated, and *Dnmt3a* deficiency did not cause a genome-wide variation in DNA methylation (Fig. 4f). Thus, we performed a genome-wide search for genomic regions with differences in cytosine methylation ('differentially methylated regions' (DMRs)) in the cytosine-guanine context in *Dnmt3a*-sufficient peritoneal macrophages versus *Dnmt3a*-deficient peritoneal macrophages, naive *Dnmt3a*-sufficient peritoneal macrophages versus their LPS-stimulated counterparts, or naive *Dnmt3a*-sufficient peritoneal macrophages versus their VSV-infected counterparts and found hundreds of DMRs in each of the pairs analyzed (Supplementary Table 3). We then analyzed the DNA-methylation variation trends of the DMRs for each of those pairs and found that the proportion of DMRs with downregulated DNA methylation before and after VSV infection or LPS stimulation in *Dnmt3a*-deficient peritoneal macrophages relative to that in *Dnmt3a*-sufficient peritoneal macrophages was greater than the proportion of DMRs with upregulated DNA methylation before and after VSV infection or LPS stimulation in *Dnmt3a*-deficient peritoneal macrophages relative to that in *Dnmt3a*-sufficient peritoneal macrophages (Fig. 4g). For the dynamic DNA methylomes of VSV-infected or LPS-stimulated peritoneal macrophages, hundreds of DMRs were also found in these cells as well (Fig. 4g). A large fraction of the DMRs were located in gene regions (Fig. 4h), which indicated that *Dnmt3a*-mediated methylation of DNA might regulate gene transcription. Using the methylome data, we further analyzed methylation of the same region detected above at the distal *Hdac9* promoter and also found



downregulated methylation at the distal *Hdac9* promoter before and after VSV infection or LPS stimulation in *Dnmt3a*-deficient peritoneal macrophages, relative to its methylation in their *Dnmt3a*-sufficient counterparts (Fig. 4i).

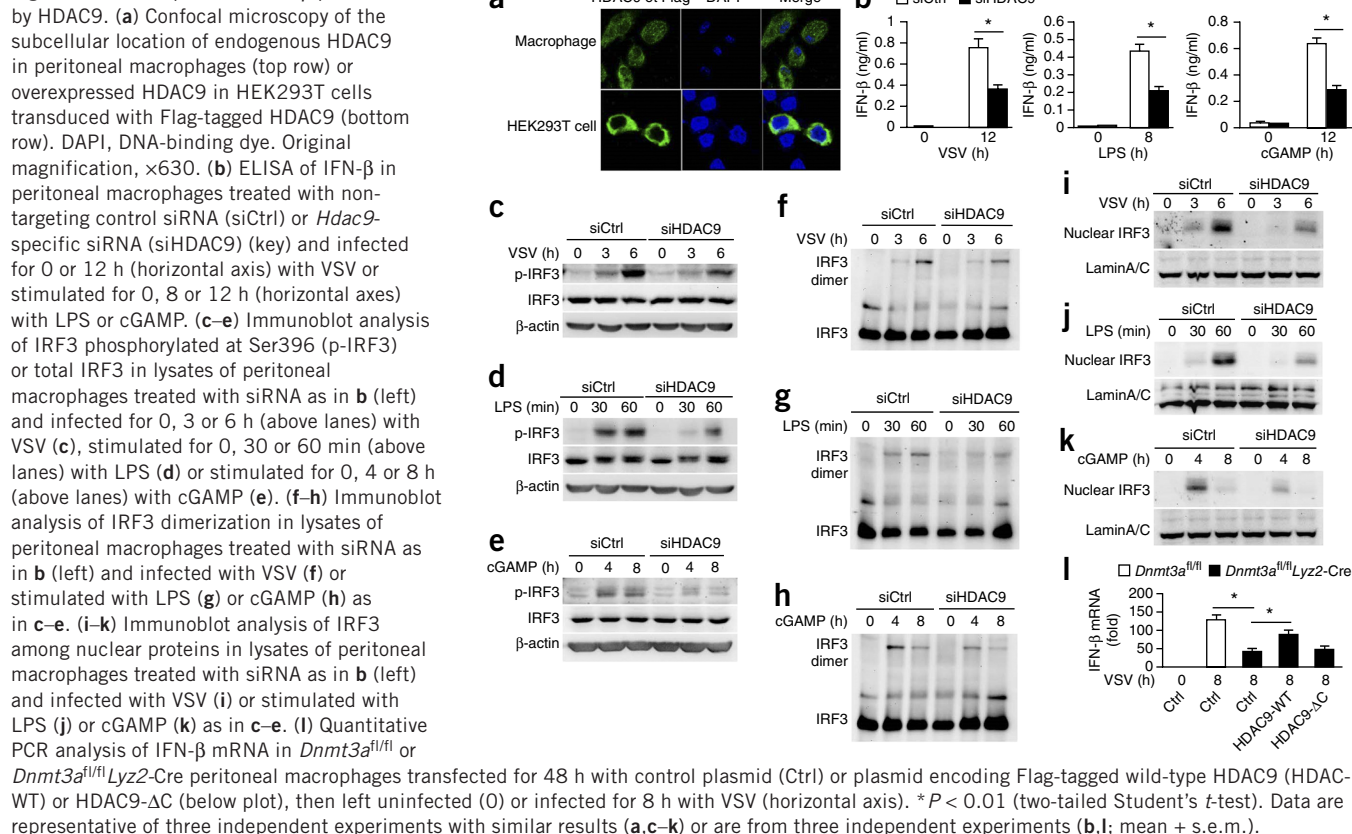
Deficiency in or knockdown of *Dnmt3a* increased the abundance of H3K27me3 at the distal promoter region of *Hdac9* (Fig. 4j,k). Furthermore, we assessed EZH2, a histone methylase that catalyzes the addition of methyl groups to histone H3 at Lys27 (ref. 30), and found that the binding of EZH2 to the distal promoter region of *Hdac9* was greater in *Dnmt3a*-deficient peritoneal macrophages than in their *Dnmt3a*-sufficient counterparts (Fig. 4l). We also detected activating histone marks at the distal and proximal promoters of *Hdac9* and found that although ‘downregulated’ H3K4me3 marks were present in the distal *Hdac9* promoter in *Dnmt3a*-deficient peritoneal macrophages, much lower signals were present in the distal promoter than in the proximal promoter (Fig. 4m). Furthermore, we assessed the acetylation of histone H3 (H3Ac) and found much higher H3Ac signals in the proximal *Hdac9* promoter than in the distal *Hdac9* promoter and that *Dnmt3a* deficiency significantly decreased the H3Ac signals at the proximal *Hdac9* promoter (Fig. 4n). These results indicated that *Dnmt3a*-mediated methylation at the distal *Hdac9* promoter increased its transcription mainly through repression of

the repressive histone mark H3K27me3. Together these results suggested that *Dnmt3a* maintained high expression of HDAC9 in peritoneal macrophages.

Dnmt3a promotes IFN- β production by HDAC9

We then set out to determine whether HDAC9 was involved in regulating the phosphorylation of IRF3 and production of IFN- β . By detecting the subcellular location of endogenous HDAC9 in peritoneal macrophages and overexpressed HDAC9 in HEK293T human embryonic kidney cells, we found HDAC9 was located mainly in the cytoplasm (Fig. 5a). To further exclude the possibility that HDAC9 might regulate transcription during PRR signaling, we performed microarray and KEGG analysis of naive peritoneal macrophages in which the gene encoding HDAC9 was silenced and found that knockdown of HDAC9 barely decreased the transcription of genes encoding transducers and regulators of PRR signaling. Transcription of only the genes encoding ISG15, the E3 ubiquitin ligase Trim25 and the transcription factor IRF7 was upregulated in naive peritoneal macrophages in which HDAC9 was knocked down, probably due to feedback of impaired TBK1-IRF3 signaling (Supplementary Table 4).

Next we investigated the role of HDAC9 in regulating the production of type I interferons. Knockdown of HDAC9 in peritoneal

Figure 5 Dnmt3a promotes IFN- β production by HDAC9.

macrophages (Supplementary Fig. 5a,b) significantly inhibited the expression IFN- β (both mRNA and protein) induced by VSV, LPS or cGAMP, but not that of TNF or IL-6 (Fig. 5b and Supplementary Fig. 5c). These data indicated that HDAC9 was required for IFN- β expression. Finally, we investigated the role of HDAC9 in regulating the phosphorylation of IRF3. Knockdown of HDAC9 in peritoneal macrophages suppressed the phosphorylation of IRF3 at Ser396 induced by VSV, LPS or cGAMP (Fig. 5c–e). Similarly, dimerization of IRF3 was also lower in peritoneal macrophages in which HDAC9 was knocked down that were then infected with VSV or stimulated with LPS or cGAMP than in similarly treated cells in which HDAC9 was not knocked down (Fig. 5f–h). Knockdown of HDAC9 resulted in less VSV-, LPS- or cGAMP-induced translocation of IRF3 to the nucleus (Fig. 5i–k). Moreover, the impaired transcription of IFN- β mRNA in *Dnmt3a*-deficient peritoneal macrophages induced by infection with VSV was ‘rescued’ by overexpression of wild-type HDAC9 but not by overexpression of an HDAC9 mutant with deletion of its deacetylation domain (HDAC9- Δ C) (Fig. 5l). Together these data indicated that Dnmt3a promoted IFN- β production and IRF3 phosphorylation mainly through HDAC9 and probably in an acetylation-dependent manner.

HDAC9 interacts with TBK1 via the deacetylase domain

We analyzed the network of binding partners that interact with HDAC9 (its ‘interactome’) by co-immunoprecipitation coupled with mass spectrometry to search for HDAC9-binding partners among PRRs and signaling transducers in the KEGG database and identified TBK1, CD14, STAT1, Ddx3x, Dhx58, Map3k1 and Trim25. Only TBK1 was the signal transducer common to TLR3, TLR4, the RNA helicase and cytosolic receptor RIG-I and STING, but not the

TLR9-related pathway for activating IRF3 (data not shown). TBK1 has a key role in integrating innate-receptor signaling and phosphorylates IRF3, IRF7 and other target proteins³¹. We sought to determine whether HDAC9 in the cytoplasm was able to interact with and activate TBK1. The endogenous HDAC9-TBK1 complex was detected in peritoneal macrophages even in the absence of VSV infection; however, this interaction was enhanced in the presence of VSV infection (Fig. 6a). Furthermore, when we overexpressed Myc-tagged TBK1 and Flag-tagged HDAC9 in HEK293T human embryonic kidney cells, immunoprecipitation experiments showed that HDAC9 was able to interact with TBK1 (Fig. 6b). To determine how TBK1 interacted with HDAC9, we constructed TBK1 mutants with deletion of various domains (Fig. 6c) and found that the ubiquitin-like domain and coiled-coil domains of TBK1 were required for the interaction of TBK1 with HDAC9 (Fig. 6d). To investigate whether the deacetylation activity of HDAC9 had a critical role in promoting TBK1 activation, we transfected vector encoding the HDAC9- Δ C mutant (lacking the deacetylation domain) into HEK293T cells together with vector encoding Myc-tagged TBK1. Co-immunoprecipitation revealed that the carboxy-terminal part of the deacetylation domain of HDAC9 was necessary for the interaction of HDAC9 and TBK1 (Fig. 6e), which indicated that the deacetylase domain of HDAC9 was required for formation of the HDAC9-TBK1 complex and that acetylation might be involved in the interaction of HDAC9 with TBK1.

HDAC9 directly enhances the kinase activity

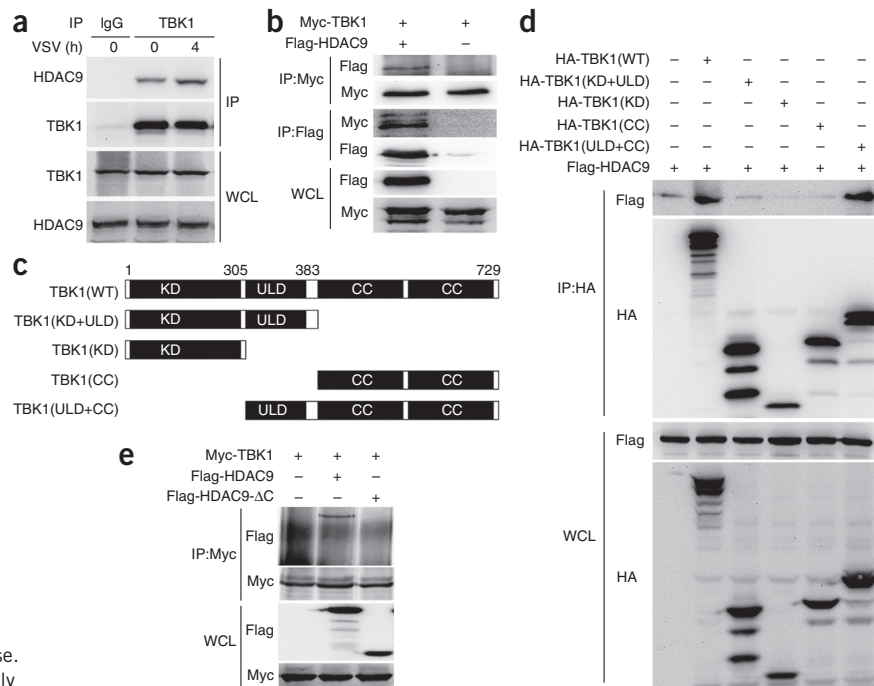
The observation that the deacetylase domain of HDAC9 was required for the interaction of HDAC9 with TBK1 indicated that HDAC9-catalyzed deacetylation of lysine residues of TBK1 might be involved in regulating activation of the kinase activity of TBK1. We assessed the

Figure 6 HDAC9 interacts with TBK1 via the HDAC9 deacetylase domain. (a) Immunoblot analysis of endogenous HDAC9 or TBK1 in peritoneal macrophages infected for 0 or 4 h (above lanes) with VSV, assessed before (whole-cell lysates (WCL); bottom) or after (IP; top) immunoprecipitation with IgG (control) or antibody to TBK1 (top).

(b) Immunoblot analysis of HDAC9 or TBK1 in HEK293T cells transfected to overexpress Myc-tagged TBK1 alone or together with Flag-tagged HDAC9 (above lanes), assessed before (WCL) or after (IP) immunoprecipitation with antibody to Myc or Flag (left margin).

(c) Structure of wild-type TBK1 (top), showing the kinase domain (KD), ubiquitin-like domain (ULD) and coiled-coil domains (CC), and mutant TBK1 (below) containing various combinations of those domains (left margin); numbers above indicate positions of amino acids. (d) Immunoblot analysis of HEK293T cells transiently transfected for 48 h with vector encoding hemagglutinin (HA)-tagged wild-type or mutant TBK1 (as in c) plus vector encoding Flag-tagged HDAC9 (above lanes), assessed before (WCL) or after (IP) immunoprecipitation with anti-hemagglutinin agarose.

(e) Immunoblot analysis of HEK293T cells transiently transfected for 48 h with vector encoding Myc-tagged TBK1 together with vector encoding Flag-tagged wild-type HDAC9 or HDAC9-ΔC (above lanes), assessed before (WCL) or after (IP) immunoprecipitation with anti-Myc agarose. Data are representative of three independent experiments with similar results.

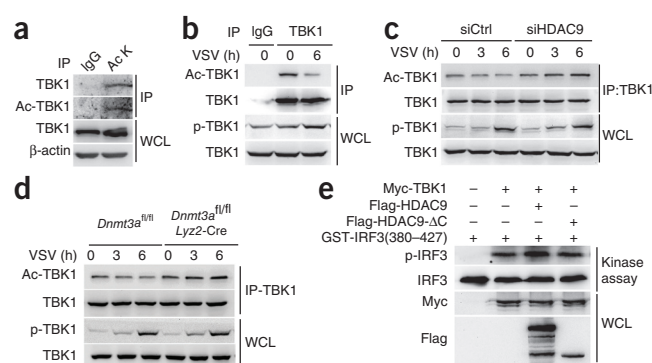


acetylation of lysine residues in endogenous TBK1 immunoprecipitated from whole-cell extracts of mouse peritoneal macrophages in the absence of innate stimuli by using an antibody to all acetylated lysines and found that endogenous TBK1 was indeed acetylated (Fig. 7a). We observed lysine-acetylation of TBK1 immunoprecipitated from whole-cell extracts of mouse peritoneal macrophages infected with VSV and found that this acetylation decreased in the presence of VSV infection (Fig. 7b). Next, to investigate whether the acetylation of TBK1 was regulated by HDAC9, we silenced the gene encoding HDAC9 and then assessed the acetylation of TBK1. We found knock-down of HDAC9 resulted in upregulation of the acetylation of TBK1 in peritoneal macrophages even in the absence of VSV infection; however, this upregulation was enhanced in the presence of VSV infection (Fig. 7c). Similarly, the acetylation of TBK1 also increased markedly in *Dnmt3a^{fl/fl}* *Lyz2-Cre* peritoneal macrophages after infection with VSV

(Fig. 7d). Thus, HDAC9-mediated deacetylation of TBK1 was able to promote the kinase activity of TBK1 during viral infection.

To further investigate the effect of HDAC9 on promoting the enzyme activity of TBK1, we fused a peptide of IRF3 amino acids 380–427 (a known substrate of TBK1) at its carboxyl terminus to glutathione S-transferase (GST) and introduced this fusion protein into an immunoprecipitated complex containing overexpressed Flag-tagged HDAC9 and Myc-tagged TBK1. Immunoblot analysis with antibody to IRF3 phosphorylated at Ser396 showed that the phosphorylation of IRF3 by TBK1 was enhanced in the presence of wild-type HDAC9 but not in the presence of the HDAC9-ΔC mutant (Fig. 7e). Similar quantities of TBK1 were immunoprecipitated in each reaction (data not shown). We concluded that deacetylation of TBK1 via HDAC9 was able to directly enhance activation of the kinase activity of TBK1.

Figure 7 HDAC9 directly enhances activation of the kinase activity of TBK1. (a) Immunoblot analysis of endogenous total TBK1 and acetylated TBK1 (Ac-TBK1) in naive mouse peritoneal macrophages, assessed before (WCL) or after (IP) immunoprecipitation with IgG (control) or antibody to all acetylated lysine residues (Ac K). (b) Immunoblot analysis of acetylated and total TBK1 in peritoneal macrophages infected for 0 or 6 h (above lanes) with VSV, followed by immunoprecipitation with IgG or antibody to TBK1 (top; IP), and immunoblot analysis of phosphorylated (p-) and total TBK1 in lysates of those cells without immunoprecipitation (below; WCL). (c) Immunoblot analysis of acetylated and total TBK1 in peritoneal macrophages treated with control or *Hdac9*-specific siRNA (top) and infected for 0, 3 or 6 h (above lanes) with VSV, followed by immunoprecipitation with antibody to TBK1 (top; IP); below (WCL), as in b. (d) Immunoblot analysis of acetylated and total TBK1 in *Dnmt3a^{fl/fl}* or *Dnmt3a^{fl/fl}* *Lyz2-Cre* peritoneal macrophages infected for 0, 3 or 6 h (above lanes) with VSV, followed by immunoprecipitation as in c (top); below (WCL), as in b. (e) *In vitro* kinase assay of IRF3 phosphorylated at Ser396 (p-IRF3) and total IRF3 in HEK293T cells transfected to express GST-fused IRF3 peptide (GST-IRF3(380–427)) as the substrate and various combinations (above lanes) of Myc-tagged TBK1 and Flag-tagged wild-type HDAC9 or HDAC9-ΔC, assessed by immunoblot analysis of proteins immunoprecipitated with antibody to Myc or GST-fused IRF3 peptide (top); below (WCL), immunoblot analysis of Myc-tagged TBK1 or Flag-tagged HDAC9 in lysates of the cells above without immunoprecipitation. Data are representative of three independent experiments with similar results.



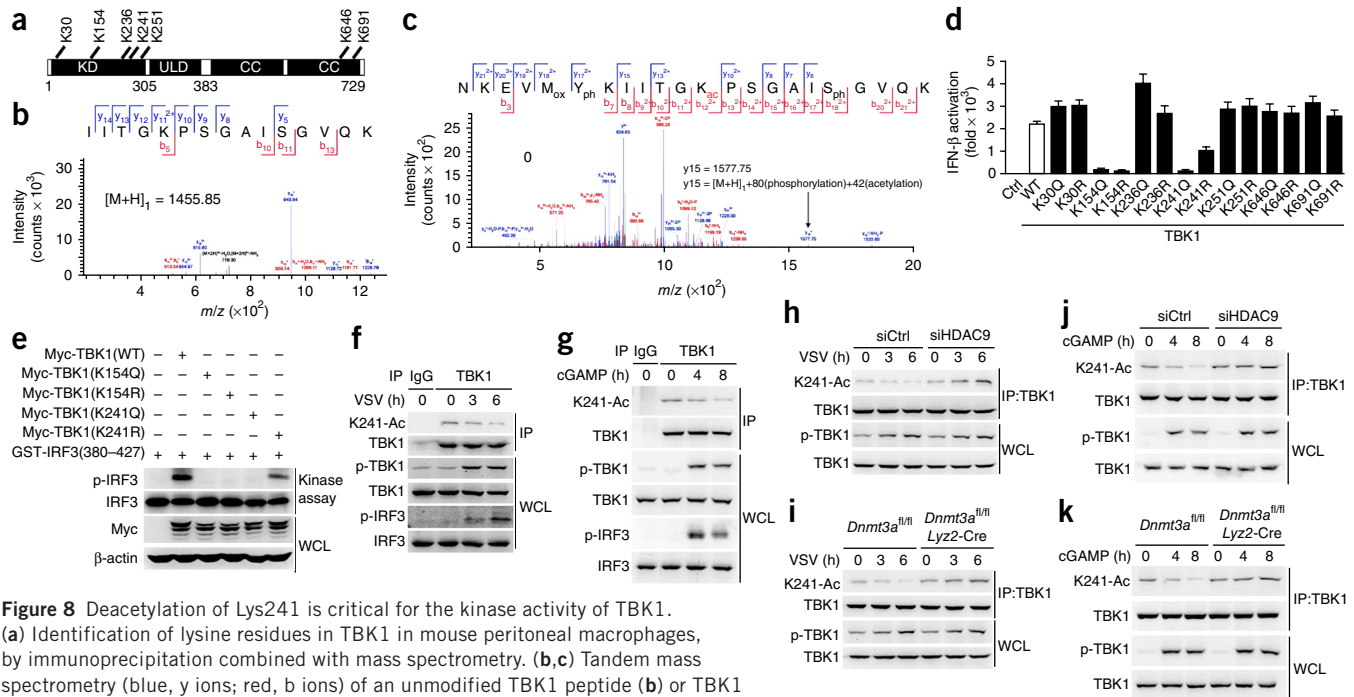


Figure 8 Deacetylation of Lys241 is critical for the kinase activity of TBK1. (a) Identification of lysine residues in TBK1 in mouse peritoneal macrophages, by immunoprecipitation combined with mass spectrometry. (b,c) Tandem mass spectrometry (blue, y ions; red, b ions) of an unmodified TBK1 peptide (b) or TBK1 peptide modified with acetylation at a lysine residue (Kac) (c); several major peaks on the spectrum were assumed to be generated by internal cleavage; acetylation is characterized by a neutral loss of 42 Da (neutral losses of H₂O or NH₃ omitted for clarity). (d) Luciferase activity of an IFN-β reporter in HEK293T cells transfected with control vector (Ctrl) or vector encoding wild-type (WT) or mutant TBK1 (horizontal axis), assessed by dual-luciferase assay; results are presented relative to those of cells transfected with control vector, set as 1. (e) *In vitro* kinase assay (as in Fig. 7e) of phosphorylated and total IRF3 in lysates of HEK293T cells transfected to express GST-fused IRF3 peptide and various combinations (above lanes) of Myc-tagged wild-type or mutant TBK1 (above), and immunoblot analysis of Myc-tagged TBK1 or β-actin in the cells above without immunoprecipitation (below; WCL). (f,g) Immunoblot analysis of TBK1 acetylated at Lys241 (K241-Ac) and total TBK1 in peritoneal macrophages infected for 0, 3 or 6 h (above lanes) with VSV (f) or stimulated for 0, 4 or 8 h (above lanes) with cGAMP (g), followed by immunoprecipitation with IgG or antibody to TBK1 (above; IP), and immunoblot analysis of phosphorylated or total TBK1 or IRF3 in the cells above without immunoprecipitation (below; WCL). (h,j) Immunoblot analysis of acetylated and total TBK1 (as in f,g) in peritoneal macrophages treated with control or *Hdac9*-specific siRNA (top) and infected with VSV or stimulated with cGAMP as in f,g, followed by immunoprecipitation with antibody to TBK1 (above; IP), and immunoblot analysis of phosphorylated or total TBK1 in the cells above without immunoprecipitation (below; WCL). (i,k) Immunoblot analysis of Lys241 acetylation in TBK1 and total TBK1 in *Dnmt3a^{fl/fl}* and *Dnmt3a^{fl/fl} Lyz2-Cre* peritoneal macrophages infected with VSV or stimulated with cGAMP as in f,g, followed by immunoprecipitation with antibody to TBK1 (above; IP); below (WCL), as in h,j. Data are representative of three independent experiments with similar results (b,c,e–k) or are from three independent experiments (d; mean + s.e.m.).

Lys241 deacetylation is critical for TBK1's kinase activity

To identify definitively acetylated lysine residues in TBK1, we used antibody to TBK1 to purify endogenous TBK1 from whole-cell extracts of *Dnmt3a^{fl/fl} Lyz2-Cre* peritoneal macrophages infected with VSV. Mass spectrometry of VSV-infected, *Dnmt3a*-deficient peritoneal macrophages indicated that seven lysine residues of TBK1 were modified by acetylation: Lys30, Lys154, Lys236, Lys241, Lys251, Lys646 and Lys691 (Fig. 8a and Supplementary Table 5). Mass spectrometry spectra indicating acetylation at Lys241 of TBK1 in VSV-infected *Dnmt3a*-deficient peritoneal macrophages served as a representative example (Fig. 8b,c). Among these acetylation sites in TBK1, Lys30 and Lys154 are two sites at which TBK1 undergoes Lys63 (K63)-linked polyubiquitination and are critical for full activation of TBK1 during innate antiviral responses and interferon production^{32,33}. However, the degree of K63-linked polyubiquitination of endogenous TBK1 in peritoneal macrophages in response to VSV infection was not substantially different in *Dnmt3a*-deficient cells versus *Dnmt3a*-sufficient cells (Supplementary Fig. 6a). Furthermore, we found that overexpression of *Dnmt3a* barely affected the polyubiquitination of TBK1 in HEK293T cells expressing hemagglutinin-tagged ubiquitin (Supplementary Fig. 6b). Collectively, these data showed that loss of *Dnmt3a* affected the acetylation of TBK1 but not its polyubiquitination.

We then sought to determine whether the acetylation sites of TBK1 noted above were able to regulate the kinase activity of TBK1. We transfected HEK293T cells with vector encoding wild-type or mutant TBK1 and then detected activation of IFN-β through a luciferase reporter assay. These mutants had replacement of the lysine at position 30, 154, 236, 241, 251, 646 or 691 with glutamine (K30Q, K154Q, K236Q, K241Q, K251Q, K646Q or K691Q) or arginine (K30R, K154R, K236R, K241R, K251R, K646R or K691R) to mimic the acetylated or nonacetylated state of the lysine residue. We found that the K154Q and K154R TBK1 mutants were unable to promote activation of the IFN-β luciferase reporter (Fig. 8d). The K241Q mutant was similar to the K154Q mutant and almost completely lacked the ability to activate IFN-β, whereas the K241R was different from the K154R mutant and still retained partial ability to activate the IFN-β luciferase reporter (Fig. 8d). Thus, Lys241 was critical for the kinase activity of TBK1, and acetylation of Lys241 impaired the kinase activity of TBK1.

To investigate whether deacetylation of Lys241 was critical for the kinase activity of TBK1, we transfected HEK293T cells with vector encoding wild-type or mutant TBK1 (K154Q, K154R, K241Q or K241R). We found that the K241R TBK1 mutant was able to mediate *in vitro* phosphorylation of the GST-IRF3 peptide substrate described above (Fig. 8e). However, the K241Q substitution resulted in a nearly complete loss of the kinase activity of

TBK1 (**Fig. 8e**). Thus, mimicking the acetylated state of Lys241 in TBK1 impaired its kinase activity.

To further confirm the role of acetylation of Lys241 in the kinase activity of TBK1, we generated an antibody directed specifically against TBK1 acetylated at Lys241. Dot-blot analysis indicated that this antibody specifically recognized TBK1 peptide acetylated at Lys241 but did not recognize a control peptide (**Supplementary Fig. 7**). By using this antibody, we analyzed Lys241-acetylated TBK1 immunoprecipitated from whole-cell extracts of peritoneal macrophages; we found Lys241-acetylated TBK1 in peritoneal macrophages and found that the acetylation of TBK1 at Lys241 was diminished after infection with VSV or stimulation with cGAMP (**Fig. 8f,g**). Moreover, knockdown of HDAC9 upregulated the acetylation of TBK1 at Lys241 in peritoneal macrophages, and the upregulation of such acetylation was greater after VSV infection (**Fig. 8h**). Similarly, the acetylation of TBK1 at Lys241 increased markedly in *Dnmt3a^{fl/fl}*Lyz2-Cre peritoneal macrophages in response to infection with VSV (**Fig. 8i**). Accordingly, knockdown of HDAC9 upregulated the acetylation of TBK1 at Lys241 in peritoneal macrophages, and the upregulation of such acetylation was greater after stimulation with cGAMP (**Fig. 8j**). Similarly, the acetylation of TBK1 at Lys241 increased markedly in *Dnmt3a^{fl/fl}*Lyz2-Cre peritoneal macrophages in response to stimulation with cGAMP (**Fig. 8k**). Together these results suggested that the deacetylation of Lys241 in TBK1 was critical for its kinase activity. Collectively, we have demonstrated that Dnmt3a enhanced the TLR3-, TLR4- or virus-induced production of type I interferons by increasing the kinase activity of TBK1 through upregulating transcription of the gene encoding HDAC9 and promoting HDAC9-mediated deacetylation of TBK1 (**Supplementary Fig. 8**).

DISCUSSION

We have shown here that Dnmt3a maintained high expression of HDAC9 in a DNA-methylation-dependent manner in naive peritoneal macrophages, which epigenetically prepared these cells for full activation of TBK1-IRF3 signaling and the production of type I interferons after viral infection. Our findings indicated that a chromatin regulator was able to establish a macrophage-specific function for rapid antiviral responses. Our findings provide new insight into how a chromatin regulator such as Dnmt3a can influence TBK1 activation and antiviral responses.

The methylation of mammalian genomic DNA is catalyzed by DNA methyltransferases, which are involved mainly in chromatin remodeling and the regulation of gene expression for the establishment of specific cell identity³⁴. CpG densities define the chromatin accessibility of the promoters of genes encoding inflammatory cytokines and determine their transcriptional kinetics during pathogen infection³⁵, and DNA methylation is stable in peritoneal macrophages during pathogen infection³⁶. However, we demonstrated that Dnmt3a-mediated DNA methylation was able to prepare macrophages for rapid and strong activation after viral infection through the regulation of transcription in resident macrophages. Furthermore, our mechanistic study of regulation revealed that DNA methylation was able to indirectly regulate the activation of a signal transducer through cross-talk with cytoplasmic histone modifiers, which would suggest that chromatin regulators not only define transcriptional activity but also indirectly determine the function of cytoplasmic proteins through the regulation of unconventional PTMs in innate immunity.

Positive and negative regulatory roles for DNA methyltransferases in viral infection have been revealed by several studies. Dnmt3a acts as a host factor required for effective HSV-1 infection³⁷, and Dnmt1 and Dnmt3b are required for the propagation of hepatitis C virus³⁸. DNA methyltransferases also methylate viral DNA, which leads to

decreased infection with hepatitis B virus³⁹. However, most of those studies focused on the regulation of viral replication by DNA methylation or its interaction with viral components for chronic viral infection. Instead, we focused on the role of methyltransferase activity in intrinsic antiviral innate signaling. Impaired production of type I interferons due to loss of Dnmt3a led to decreased induction of interferon-stimulated genes, which encode products that act against viruses at multiple levels. Further study will be needed to determine whether downregulation of Dnmt3a is an important means of escape from the immune system during pathogen infection. Moreover, genes encoding products that function in innate immunity and that are regulated by Dnmt3a and DNA methylation are potential targets for drug discovery and could serve as markers for the clinical diagnosis of infection-related diseases.

While investigating the mechanism by which Dnmt3a promotes the production of type I interferons, we found that silencing the gene encoding Dnmt3a not only downregulated dozens of genes but also upregulated dozens of genes. Although greater methylation often defines lower transcriptional activity at the enhancer and proximal promoter, methylation can also maintain high expression of genes during development of both the nervous system and the endoderm⁴⁰. Our study further revealed that Dnmt3a promoted transcription by antagonizing repressive histone modification upstream of the *Hdac9* locus during an innate immune response. Our microarray data identified other potential targets of Dnmt3a and thereby suggested additional mechanisms for the Dnmt3a-mediated positive regulation of antiviral signaling.

We also detected true activating histone marks and found less H3K4me3 and H3Ac at the proximal *Hdac9* promoter after loss of Dnmt3a. Histone acetylation often reflects transcriptional activity. Moreover, repressive and activating histone-mark regulators can interact with each other for epigenetic regulation^{41,42}. Thus, the enhancement of H3K27me3 due to loss of Dnmt3a might establish a repressive chromatin status at *Hdac9*, which might lead to a decrease in H3K4me3 and H3Ac at the proximal *Hdac9* promoter.

Unlike class I HDACs, which reside in the nucleus and deacetylate histones, class IIa HDACs such as HDAC9 (studied here) shuttle between the nucleus and cytoplasm. Export from the nucleus prevents class IIa HDACs from acting as transcriptional repressors and thus results in inducible gene expression. In some cases, class IIa HDACs can also act as transcriptional activators, but in either situation, these enzymes control gene expression mainly by recruiting other proteins (corepressors or coactivators)⁴³. HDACs can act as both positive regulators and negative regulators of TLR signaling in innate immunity, as shown by the opposing effects of HDAC inhibitors on the expression of TLR target genes^{44,45}. In antiviral signaling, beyond the class I HDACs HDAC1 and HDAC8, which repress the transcription of IFN- β mRNA, the class IIb HDAC HDAC6 activates IFN- β expression and mediates the deacetylation of β -catenin to promote IRF3-activated transcription^{46,47}. However, those studies used mainly primary epithelial cells and tumor cell lines. Here we found that high expression of cytoplasmic HDAC9 (a class IIa HDAC) resulted in promotion of the kinase activity of TBK1 via maintenance of the deacetylation status of TBK1 in primary peritoneal macrophages during viral infection. Moreover, we identified an HDAC as a regulator of the activation of a signal transducer (TBK1) in the cytoplasm during an innate immune response.

PTMs can be critical for optimizing signal transduction during innate immune responses. Several PTMs of TBK1 induced by innate signals have been identified. Autophosphorylation of TBK1 at Ser172 and K63-linked polyubiquitination of TBK1 are essential for its activation^{18,25}. Modification at Lys694 of TBK1 with the small ubiquitin-like modifier SUMO contributes to adaptor binding for the transduction of antiviral signaling⁴⁸. Furthermore, the kinase activity of TBK1 is also

regulated through protein interaction, chemical compounds and hormones in a PTM-independent manner⁴⁹. We found that acetylation was involved in regulating the activation of TBK1 and that deacetylation of Lys241 in TBK1 was critical for its kinase activity independently of the reported conventional PTMs of TBK1. The underlying mechanism for this might be that the charge state and structure of TBK1 is altered by acetylation thus its catalytic activity is also altered. Furthermore, our results also indicated the possibility that certain histone acetyltransferases might act as negative regulators of TBK1 activation during pathogen infection; however, this requires further investigation.

METHODS

Methods and any associated references are available in the [online version of the paper](#).

Accession codes. GEO: microarray and deep sequencing data, [GSE69256](#), [GSE70631](#) and [GSE74750](#).

Note: Any Supplementary Information and Source Data files are available in the online version of the paper.

ACKNOWLEDGMENTS

We thank J. Zhu and N. Wang for mass-spectrometry analysis; Z. Chen (University of Texas Southwestern Medical Center) for the L929-shSTING cell line; B. Sun (Chinese Academy of Sciences) for SeV; and Q. Li (Chinese Academy of Medical Sciences) for HSV-1 virus (Kos strain). Supported by the National Key Basic Research Program of China (2013CB530502) and National Natural Science Foundation of China (31390431, 31370864 and 31200654).

AUTHOR CONTRIBUTIONS

X. Li, Q.Z. Y.D., Y.L., D.Z., K.Z., Q.S., X. Liu, X.Z., N.L. and Q.W. performed the experiments; Q.Z. established the DNA methylomes and performed bioinformatics analysis; Z.C. did mass-spectrometry analysis; G.F. provided *Dnmt3a*^{fl/fl} mice; X.C. designed and supervised the research; and X.C., X. Li, Q.Z. and Q.W. analyzed data and wrote the manuscript.

COMPETING FINANCIAL INTERESTS

The authors declare no competing financial interests.

Reprints and permissions information is available online at <http://www.nature.com/reprints/index.html>.

1. Smale, S.T., Tarakhovsky, A. & Natoli, G. Chromatin contributions to the regulation of innate immunity. *Annu. Rev. Immunol.* **32**, 489–511 (2014).
2. Álvarez-Erro, D., Vento-Torres, R., Sieweke, M. & Ballestar, E. Epigenetic control of myeloid cell differentiation, identity and function. *Nat. Rev. Immunol.* **15**, 7–17 (2015).
3. Foster, S.L., Hargreaves, D.C. & Medzhitov, R. Gene-specific control of inflammation by TLR-induced chromatin modifications. *Nature* **447**, 972–978 (2007).
4. Saeed, S. *et al.* Epigenetic programming of monocyte-to-macrophage differentiation and trained innate immunity. *Science* **345**, 1251086 (2014).
5. Ramirez-Carrozzi, V.R. *et al.* Selective and antagonistic functions of SWI/SNF and Mi-2beta nucleosome remodeling complexes during an inflammatory response. *Genes Dev.* **20**, 282–296 (2006).
6. Zhang, Q. *et al.* Tet2 is required to resolve inflammation by recruiting Hdac2 to specifically repress IL-6. *Nature* **525**, 389–393 (2015).
7. Jones, P.A. Functions of DNA methylation: islands, start sites, gene bodies and beyond. *Nat. Rev. Genet.* **13**, 484–492 (2012).
8. Anderson, P. Post-transcriptional regulons coordinate the initiation and resolution of inflammation. *Nat. Rev. Immunol.* **10**, 24–35 (2010).
9. Mowen, K.A. & David, M. Unconventional post-translational modifications in immunological signaling. *Nat. Immunol.* **15**, 512–520 (2014).
10. Piccirillo, C.A., Bjur, E., Topisirovic, I., Sonenberg, N. & Larsson, O. Translational control of immune responses: from transcripts to translomes. *Nat. Immunol.* **15**, 503–511 (2014).
11. Verdin, E. & Ott, M. 50 years of protein acetylation: from gene regulation to epigenetics, metabolism and beyond. *Nat. Rev. Mol. Cell Biol.* **16**, 258–264 (2015).
12. Cao, W., Bao, C., Padalko, E. & Lowenstein, C.J. Acetylation of mitogen-activated protein kinase phosphatase-1 inhibits Toll-like receptor signaling. *J. Exp. Med.* **205**, 1491–1503 (2008).
13. Munshi, N. *et al.* Acetylation of HMG I(Y) by CBP turns off IFN beta expression by disrupting the enhancosome. *Mol. Cell* **2**, 457–467 (1998).
14. Nuszon, I. & Horvath, C.M. Interferon-stimulated transcription and innate antiviral immunity require deacetylase activity and histone deacetylase 1. *Proc. Natl. Acad. Sci. USA* **100**, 14742–14747 (2003).
15. Fitzgerald, K.A. *et al.* IKKepsilon and TBK1 are essential components of the IRF3 signaling pathway. *Nat. Immunol.* **4**, 491–496 (2003).
16. Liu, S. *et al.* Phosphorylation of innate immune adaptor proteins MAVS, STING, and TRIF induces IRF3 activation. *Science* **347**, aaa2630 (2015).
17. Cao, X. Self-regulation and cross-regulation of pattern-recognition receptor signalling in health and disease. *Nat. Rev. Immunol.* **16**, 35–50 (2016).
18. Wang, C. *et al.* The E3 ubiquitin ligase Nrdp1 'preferentially' promotes TLR-mediated production of type I interferon. *Nat. Immunol.* **10**, 744–752 (2009).
19. Li, S., Wang, L., Berman, M., Kong, Y.Y. & Dorf, M.E. Mapping a dynamic innate immunity protein interaction network regulating type I interferon production. *Immunity* **35**, 426–440 (2011).
20. Cui, J. *et al.* NLRP4 negatively regulates type I interferon signaling by targeting the kinase TBK1 for degradation via the ubiquitin ligase DTX4. *Nat. Immunol.* **13**, 387–395 (2012).
21. Wu, C., Macleod, I. & Su, A.I. BioGPS and MyGene.info: organizing online, gene-centric information. *Nucleic Acids Res.* **41**, D561–D565 (2013).
22. Chen, W. *et al.* Induction of Siglec-G by RNA viruses inhibits the innate immune response by promoting RIG-I degradation. *Cell* **152**, 467–478 (2013).
23. Servant, M.J. *et al.* Identification of the minimal phosphoacceptor site required for in vivo activation of interferon regulatory factor 3 in response to virus and double-stranded RNA. *J. Biol. Chem.* **278**, 9441–9447 (2003).
24. Chau, T.L. *et al.* Are the IKKs and IKK-related kinases TBK1 and IKK-ε similarly activated? *Trends Biochem. Sci.* **33**, 171–180 (2008).
25. Ma, X. *et al.* Molecular basis of Tank-binding kinase 1 activation by transautophosphorylation. *Proc. Natl. Acad. Sci. USA* **109**, 9378–9383 (2012).
26. Wu, H. *et al.* Dnmt3a-dependent nonpromoter DNA methylation facilitates transcription of neurogenic genes. *Science* **329**, 444–448 (2010).
27. Kanehisa, M., Goto, S., Sato, Y., Furumichi, M. & Tanabe, M. KEGG for integration and interpretation of large-scale molecular data sets. *Nucleic Acids Res.* **40**, D109–D114 (2012).
28. Jones, P.L. *et al.* Methylated DNA and MeCP2 recruit histone deacetylase to repress transcription. *Nat. Genet.* **19**, 187–191 (1998).
29. Nan, X. *et al.* Transcriptional repression by the methyl-CpG-binding protein MeCP2 involves a histone deacetylase complex. *Nature* **393**, 386–389 (1998).
30. Viré, E. *et al.* The Polycomb group protein EZH2 directly controls DNA methylation. *Nature* **439**, 871–874 (2006).
31. Clément, J.F., Meloche, S. & Servant, M.J. The IKK-related kinases: from innate immunity to oncogenesis. *Cell Res.* **18**, 889–899 (2008).
32. Tu, D. *et al.* Structure and ubiquitination-dependent activation of TANK-binding kinase 1. *Cell Rep.* **3**, 747–758 (2013).
33. Wang, L., Li, S. & Dorf, M.E. NEMO binds ubiquitinated TANK-binding kinase 1 (TBK1) to regulate innate immune responses to RNA viruses. *PLoS One* **7**, e43756 (2012).
34. Wu, H. & Zhang, Y. Reversing DNA methylation: mechanisms, genomics, and biological functions. *Cell* **156**, 45–68 (2014).
35. Ramirez-Carrozzi, V.R. *et al.* A unifying model for the selective regulation of inducible transcription by CpG islands and nucleosome remodeling. *Cell* **138**, 114–128 (2009).
36. Marr, A.K. *et al.* *Leishmania donovani* infection causes distinct epigenetic DNA methylation changes in host macrophages. *PLoS Pathog.* **10**, e1004419 (2014).
37. Rowles, D.L. *et al.* DNA methyltransferase DNMT3A associates with viral proteins and impacts HSV-1 infection. *Proteomics* **15**, 1968–1982 (2015).
38. Chen, C. *et al.* DNA methyltransferases 1 and 3B are required for hepatitis C virus infection in cell culture. *Virology* **441**, 57–65 (2013).
39. Vivekanandan, P., Daniel, H.D., Kannangai, R., Martinez-Murillo, F. & Torbenson, M. Hepatitis B virus replication induces methylation of both host and viral DNA. *J. Virol.* **84**, 4321–4329 (2010).
40. Bahar Halpern, K., Vana, T. & Walker, M.D. Paradoxical role of DNA methylation in activation of FoxA2 gene expression during endodermal development. *J. Biol. Chem.* **289**, 23882–23892 (2014).
41. Zhou, W.W., Goren, A. & Bernstein, B.E. Charting histone modifications and the functional organization of mammalian genomes. *Nat. Rev. Genet.* **12**, 7–18 (2011).
42. Northrup, D.L. & Zhao, K. Application of ChIP-Seq and related techniques to the study of immune function. *Immunity* **34**, 830–842 (2011).
43. Shakespear, M.R., Halili, M.A., Irvine, K.M., Fairlie, D.P. & Sweet, M.J. Histone deacetylases as regulators of inflammation and immunity. *Trends Immunol.* **32**, 335–343 (2011).
44. Aung, H.T. *et al.* LPS regulates proinflammatory gene expression in macrophages by altering histone deacetylase expression. *FASEB J.* **20**, 1315–1327 (2006).
45. Halili, M.A. *et al.* Differential effects of selective HDAC inhibitors on macrophage inflammatory responses to the Toll-like receptor 4 agonist LPS. *J. Leukoc. Biol.* **87**, 1103–1114 (2010).
46. Nuszon, I. & Horvath, C.M. Positive and negative regulation of the innate antiviral response and beta interferon gene expression by deacetylation. *Mol. Cell Biol.* **26**, 3106–3113 (2006).
47. Zhu, J., Coyne, C.B. & Sarkar, S.N. PKC alpha regulates Sendai virus-mediated interferon induction through HDAC6 and β-catenin. *EMBO J.* **30**, 4838–4849 (2011).
48. Saul, V.V., Niedenthal, R., Pich, A., Weber, F. & Schmitz, M.L. SUMO modification of TBK1 at the adaptor-binding C-terminal coiled-coil domain contributes to its antiviral activity. *Biochim. Biophys. Acta* **1853**, 136–143 (2015).
49. Zhao, W. Negative regulation of TBK1-mediated antiviral immunity. *FEBS Lett.* **587**, 542–548 (2013).

ONLINE METHODS

Mice. *Lyz2-Cre* mice on the C57BL/6 background were from Jackson Laboratories. C57BL/6 male mice 6–8 weeks of age were purchased from Joint Ventures Sipper BK Experimental Animals (Shanghai, China). Mice were kept and bred in pathogen-free conditions. All animal experiments were undertaken in accordance with the National Institute of Health Guide for the Care and Use of Laboratory Animals with approval of the Scientific Investigation Board of Second Military Medical University, Shanghai.

Reagents and antibodies. LPS (0111:B4), poly(I:C) and CpG ODN have been described²⁵. Kinase buffer (#9802), ATP (#9804), ChIP Grade Protein G Magnetic Beads (#9006) and Cell Lysis Buffer (#9803) were from Cell Signaling Technology. Protein G-agarose (20397) used for immunoprecipitation were from Pierce. Anti-hemagglutinin-agarose (A2095), anti-Myc-agarose (A7470), anti-Flag-agarose (A2220) used for immunoprecipitation were from Sigma. The antibodies used in this study are in **Supplementary Table 6**. The antibody directed against TBK1 acetylated at Lys241 (TBK1 K241Ac) was customized produced by Abmart (Shanghai, China). Antigenic 11aa peptide (amino acids 236–246 of TBK1) with acetylated lysine (KIITG(acK)PSGAI) and the according control peptide (KIITGKPSGAI) were designed and *in vitro* synthesized. The rabbit polyclonal antibodies to the peptides were purified using protein A.

Cells and pathogens. The HEK293T and RAW264.7 cell lines were from American Type Culture Collection. All cells were cultured in endotoxin-free DMEM (GIBCO), supplemented with 10% FCS (Invitrogen), 5 mg/ml penicillin (GIBCO) and 10 mg/ml streptomycin (GIBCO). VSV (Indiana Strain) was propagated and amplified by infection of a monolayer of HEK293T cells. 48 h after infection, the supernatant was harvested and clarified by centrifugation. Viral titer was determined by TCID₅₀ on HEK293T cells.

Isolation of macrophages. Peritoneal macrophages were harvested from mice 4 d after thioglycollate (BD, Sparks, MD) injection. Cells were plated into 12-well plates and cultured in the absence or presence of LPS (100 ng/ml), CpG ODN (0.3 μ M), Poly (I:C) (10 μ g/ml).

Virus Infection. Cells were infected with VSV (1 M.O.I.), SeV (1 M.O.I.) or HSV-1 (10 M.O.I.) for the indicated hours. Cytokine production was analyzed 12 h later. For *in vivo* cytokine production studies, age- and sex-matched groups of littermate mice were intraperitoneally infected with VSV (5×10^7 plaque-forming units per gram body weight).

RNA-mediated interference. Thioglycollate-elicited mouse peritoneal macrophages were transfected with siRNA (20nM) through use of INTERFERin reagent (Polyplus Transfection). The mouse specific siRNA targeting Dnmt3a and HDAC9 were designed and synthesized by GenePharma Co (Shanghai, China). The mouse Dnmt3a siRNA 5'-ACUCUAUAAAGCAGGGCAAUU-3', the mouse HDAC9 siRNA 5'-CUAACUCACUCAAGACAAUU-3', the nonsense sequence 5'-UUCUCCGAACGUGUCACGUTT-3' was used as control siRNA.

RNA quantification. Total RNA was extracted with Trizol reagent (Transgen) and reversed-transcribed with Reverse Transcription System (Promega). Reverse transcription products of different samples were amplified by LightCycler System (Roche) using the SYBR Green PCR Master Mix (Applied Biosystems) according to the manufacturer's instructions and data were normalized by the level of β -actin expression in each individual sample. $2^{-\Delta\Delta Ct}$ method was used to calculate relative expression changes. With the help of dissociation curve analysis and the sequencing of PCR products, pairs of specific primers of each cDNAs were designed and selected, without any primer dimers or unspecific amplification detected. The sequences of the primers for quantitative real-time RT-PCR are in **Supplementary Table 7**.

ELISA. Secreted cytokines in cell culture supernatants or sera from virus infected-mice were analyzed using mouse IFN- β and IFN- α (PBL Biomedical Laboratories), mouse TNF and IL-6 (R&D Systems) ELISA kits according to the manufacturer's instructions.

Co-immunoprecipitation and immunoblot analysis. Cells were lysed with cell lysis buffer (Cell Signaling Technology) supplemented with protease inhibitor 'cocktail'. Protein concentrations in the extracts were measured by BCA assay (Pierce). Immunoprecipitation and immunoblot analysis were done as described⁵⁰.

Microarray analysis. Total RNA was isolated using an RNA isolation kit (Qiagen) and verified with RNA integrity number (RIN). Whole genome wide expression analysis was performed with Agilent Mouse Genome Arrays (design ID:014868). Raw data were normalized by Quantile algorithm, Gene Spring Software 11.0 (Agilent technologies, Santa Clara, CA, USA).

RNA-seq analysis. Total RNA was used for mRNA isolation and cDNA library generation with the TruSeq RNA Sample Preparation Kit (Illumina Inc., San Diego, USA). Clusters were generated with the TruSeq SR Cluster Kit v2 according to the reagent preparation guide. The RNA sequencing was performed using the illuminaHiSeq 2500 platform. High-quality reads were aligned to GRCm38 using Tophat. The expression levels for each of the genes were normalized to FPKM (fragments per kilobase of transcript per million fragments mapped). Cuffdiff was used to compare mRNA levels between samples.

ChIP. These assays were done according to the protocol of the ChIP assay kit (Millipore). Target-gene promoter sequences in both input DNA and recovered DNA immunocomplexes were detected by PCR. Data were normalized to the corresponding DNA input control. The sequences of primer pairs specific for the *Ifnb1* and *Hdac9* promoter region used in this study are in **Supplementary Table 8**.

Methylated-DNA immunoprecipitation. These assays were done according to the protocol of the MeDIP kit (abcam). DNA were extracted from *Dnmt3a^{fl/fl}Lyz2-Cre* and *Dnmt3a^{fl/fl}* peritoneal macrophages, and methylated DNA fragments were immunoprecipitated via an antibody raised against 5-methylcytosine (5mC), then PCR analysis of *Hdac9* distal promoter. PCR was used to amplify the region of interest from the eluted DNA. Genomic sequences were retrieved from the UCSC genome database. The sequences of primer pairs specific for the *Hdac9* up8k promoter region used in this study as follows: *Hdac9*: forward 5'-TCAAATCAAGACCCAGTGATCC-3' and reverse 5'-GGCAGTCATTTTCATAGCTGC-3'. The sequences of primer pairs specific for the *Ifnb1* up1k promoter region used in this study as follows: *Ifnb1*: forward 5'-GCACAAGATCCTGGAATA-3' and reverse 5'-TGTGAGTGGGTAAACAGAG-3'.

Bisulfite TA clone sequencing. Genomic DNAs isolated from control and *Dnmt3a*-deficient peritoneal macrophages were bisulfite converted using the EpiTect Fast DNA Bisulfite kit (QIAGEN). PCR was used to amplify the *Hdac9* gene upstream region. The PCR primers are as follows: sense: 5'-GGGAAGG GTATTAAATTAAGATTTAGTG-3', antisense: 5'-AAATAACAATCATTTT CATAACTACTC-3'. The PCR products were sub-cloned, and 20 clones were selected and sequenced. To calculate the methylation rate of each cytosine in the CG context, we counted methylated and unmethylated cytosines of the clones covering each cytosine of the region.

Immunofluorescent confocal microscopy. The experiments were performed as described previously⁵¹. HEK293T cells plated on glass cover slips in six-well plates were cotransfected with indicated plasmids and then labeled with antibody to tag. Or peritoneal macrophages plated on glass coverslips were labeled with antibody to HDAC9. Imaging of the cells was carried out using Leica TCS SP2 confocal laser microscopy under a $\times 100$ oil objective.

Plasmid constructs and transfection. cDNA encoding mouse HDAC9 or TBK1 was amplified from peritoneal macrophages. They were cloned into pcDNA3.1-Flag or pcDNA3.1-Myc eukaryotic expression vectors respectively. Deleted, truncated and point mutants were generated by PCR-based amplification and the construct coding the wild-type protein as the template. Each construct was confirmed by sequencing. Plasmids were transiently transfected into HEK293T cells with jetPEI reagents (Polyplus Transfection) according to

the manufacturer's instructions. The sequences of PCR primers for Expressing Vectors used in this study are in **Supplementary Table 9**.

In vitro kinase assay. The experiments were performed as described previously⁵² with some modifications. HEK293T WCL (1 mg) with TBK1-Myc overexpressed were incubated for 2 h at 4 °C with anti-Myc-agarose (sigma). Immunocomplexes were washed twice with 1× cell lysis buffer (#9803s, CST) and then twice with 1× kinase buffer (#9802, CST). Kinase reactions were performed by incubation of immunocomplexes with 1× kinase buffer, 1 mM ATP (#9804, CST) and 1.0 µg purified GST-fused IRF3 peptide (amino acids 380–427) as the substrate at 30 °C for 90 min in 50-µl reaction mixture. Samples were separated by SDS-PAGE, and analyzed by immunoblotting with anti-phospho-IRF3.

Co-immunoprecipitation coupled with LC-MS/MS analysis. 1×10^8 peritoneal macrophages infected with VSV for 8 h were lysed with 10 ml Cell Lysis Buffer. Soluble fraction was subjected to immunoprecipitation with 10 µg antibody recognizing HDAC9 or IgG overnight. 100 µl protein G Magnetic beads (Cell Signaling Technology) prewashed with Cell Lysis Buffer containing 0.1% BSA were added and incubated for another 2 h at 4 °C. Protein complex-containing beads were washed with NETN (100 mM NaCl, 20 mM Tris-HCl (pH 8.0), 1 mM EDTA, 0.05% (v/v) NP-40) for four times. Proteins were eluted and boiled in 1% SDS loading buffers. After SDS-PAGE and silver staining, positions in gel lanes where there were more bands in HDAC9-group were determined. Gel pieces at these positions in both IgG- and HDAC9-group were respectively cut and subjected into in-gel digestion and LC-MS/MS analysis. The resulting MS/MS data were processed using Mascot search engine (version 3.2). Tandem mass spectra were searched against SwissProt-Mouse database concatenated with reverse decoy database. Proteins containing unique mapped peptide with ion score meeting significant P value were considered. These eligible proteins above four unique peptides of which were identified in MS analysis appeared in HDAC9-group but not in IgG-group were chosen.

Mass spectrometry analysis of lysine acetylation. Thioglycolate-elicited Dnmt3a-deficient peritoneal macrophages were infected with VSV and then lysed for immunoprecipitation with antibody to TBK1 (or with IgG as a control). After Commassie Blue staining, the TBK1 specific band with intensive signal compared with IgG control were cut and then followed by analysis by reverse-phase nanospray liquid chromatography–tandem mass spectrometry. The spectra from tandem mass spectrometry were automatically used for searching against the non-redundant International

Protein Index mouse protein database (version 3.72) with the Bioworks browser (rev.3.1).

DNA sample preparation and bisulfite sequencing. Total DNA was isolated using a QIAamp DNA Mini Kit (QIAGEN). The DNA was fragmented by sonication using a Bioruptor (Diagenode, Belgium) to a mean size of approximately 250 bp, followed by the blunt-ending, dA addition to 3'-end and, finally, adaptor addition (in this case of methylated adaptors to protect from bisulfite conversion), essentially according to the manufacturer's instructions. The bisulfite conversion of the adaptor-added DNA was carried out using EpiTect Bisulfite Kit (QIAGEN). High-throughput sequencing was performed with HiSeq 3000, and raw data were processed and methylation of cytosine residues was calculated as previously reported⁵³.

DMR searching. DMRs were identified by sliding windows containing at least three CGs. DMRs satisfying the following two standards were selected. First, difference of DNA methylation levels of the DMR was more than double between two samples (Fisher test, $P < 0.05$). Second, the DNA methylation level of the DMR in either sample was higher than 0.4. Each DMR was extended unless the distance between the two CGs was over 200 bp or the extended DMR no longer met the above standards. When the distance between the two DMRs was less than 2 kb, they were merged into one. Furthermore, DMRs which contained at least three CGs with effective coverage higher than four for each of the CGs were chosen.

Statistical analysis. Statistical significance between groups was determined by two-tailed Student's *t*-test. Differences were considered to be significant when $P < 0.05$. Sample sizes were chosen by standard methods to ensure adequate power, and no exclusion, randomization of weight and sex or blinding was used for animal studies. For mouse survival studies, Kaplan-Meier survival curves were generated and analyzed for statistical significance with GraphPad Prism 5.0.

50. Han, C. *et al.* Integrin CD11b negatively regulates TLR-triggered inflammatory responses by activating Syk and promoting degradation of MyD88 and TRIF via Cbl-b. *Nat. Immunol.* **11**, 734–742 (2010).
51. Xu, S. *et al.* Constitutive MHC class I molecules negatively regulate TLR-triggered inflammatory responses via the Fps-SHP-2 pathway. *Nat. Immunol.* **13**, 551–559 (2012).
52. Zhao, T. *et al.* The NEMO adaptor bridges the nuclear factor-κB and interferon regulatory factor signaling pathways. *Nat. Immunol.* **8**, 592–600 (2007).
53. Li, Y. *et al.* The DNA methylome of human peripheral blood mononuclear cells. *PLoS Biol.* **8**, e1000533 (2010).